International Journal of Applied Earth Observations and Geoinformation 105 (2021) 102632

Contents lists available at ScienceDirect

International Journal of Applied Earth Observations and Geoinformation

journal homepage: www.elsevier.com/locate/jag

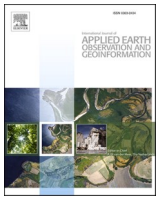

Assessing the efficiency of mitigation measures to reduce groundwater depletion and related land subsidence in Querétaro (Central Mexico) from decadal InSAR observations

Pascal Castellazzi [a,*], Jaime Garfias [b], Richard Martel [c]

[a] Commonwealth Science and Industrial Research Organisation (CSIRO), Deep Earth Imaging FSP, Land and Water, Waite Rd, Urrbrae, SA 5064, Australia
[b] Universidad Autónoma del Estado de México, Instituto Interamericano de Tecnología y Ciencias del Agua, Carretera Toluca-Atlacomulco, km 14.5, Unidad San Cayetano, C.P. 50200, Toluca, Edo. de México, Mexico
[c] Institut national de la recherche scientifique, Centre Eau Terre et Environnement, Université du Québec, 490 rue de la Couronne, Québec, QC G1K 9A9, Canada

ARTICLE INFO

Keywords:
Groundwater depletion
Groundwater management
Land subsidence
Mexico
InSAR
Ground fracture

ABSTRACT

Groundwater overexploitation occurs throughout Central Mexico and is a major threat to the sustainable development of the region. The two most direct impacts are on groundwater/surface water interactions and uneven land subsidence causing ground fracturing. The latter implies frequent and costly repairs to linear urban infrastructure such as roads or water/gas distribution conduits. In 2011, the state of Querétaro drastically changed the water management scheme to solve the groundwater depletion and ground fracturing issues in the Querétaro Valley. Groundwater extraction was decreased by half and the missing portion was replaced by water imports transported through a major 123 km-long aqueduct infrastructure. In this paper, we evaluate if this change in the water sourcing strategy has helped reducing groundwater overexploitation and the related ground fissuring. We present four consecutive radar interferometry-derived ground deformation time-series covering ~75% of the period 2004–2020. We observed that maximum ground deformation has drastically decreased by a factor of ~5 after 2011, from −25 to −50 mm/yr to ~−10 mm/yr, suggesting the effectiveness of the drastic water management change. However, while groundwater static pressure has recovered in the range [4, 10] m in the six years following the change, extraction has been constantly increasing. Interferometric observations based on Radarsat-2 and Sentinel-1 data, in 2013–2014 and 2017–2020 respectively, detect increasing subsidence rates up to ~−15 mm/yr. This suggests that the water management change only reduced the problem, and that a longer-term strategy will have to be implemented to fulfill the ever-increasing water demand in the region.

1. Introduction

Land subsidence often occurs as a result of unsustainable groundwater extraction. Groundwater storage loss and level decrease imply a hydrostatic pressure change in the aquifer. In compressible aquifer systems, typically containing high proportion of clay and/or silt either as parts of aquitards or discontinuous interbeds, the pressure change induces reconfiguration of the sediment matrix and compaction (Terzaghi, 1925; Biot 1941). Typically, compaction is partly elastic (recovered if hydrostatic levels recover, typically with a time lag) and partly inelastic (unrecoverable); the proportion of elastic vs. inelastic compaction depending on the pre-consolidation state of the sediment matrix. Compaction of the compressible matrix is visible as ground deformation at the surface. As compaction occurs in relation to spatially and temporally variable parameters, i.e. sediment compressibility, hydrostatic pressure change (related to aquifer storativity and confinement; see Castellazzi et al. 2016 for a detailed explanation) and aquifer thickness, ground level changes is also uneven and vary in time and space. Uneven aquifer compaction leads to ground fissuring, drastically affecting the structural stability of infrastructure.

Most cities of Central Mexico are facing major aquifer compaction and ground fissuring issues, and several of the most internationally known cases of groundwater-related land subsidence occur across the region: Mexico City (Osmanoğlu et al., 2011; Solano Rojas et al., 2015; Sowter et al., 2016), Toluca (Calderhead et al., 2010, 2011; Castellazzi et al., 2016, 2017); Querétaro (Pacheco et al., 2006; Castellazzi et al., 2016; Carreón-Freyre et al., 2016), Aguascalientes (Pacheco-Martínez et al., 2015a, 2015b; Cigna and Tapete, 2021), Morelia (Cigna et al.,

* Corresponding author.
E-mail addresses: Pascal.Castellazzi@csiro.au (P. Castellazzi), jgarfiass@uaemex.mx (J. Garfias), Richard.Martel@ete.inrs.ca (R. Martel).

https://doi.org/10.1016/j.jag.2021.102632
Received 9 July 2021; Received in revised form 15 November 2021; Accepted 18 November 2021
Available online 26 November 2021

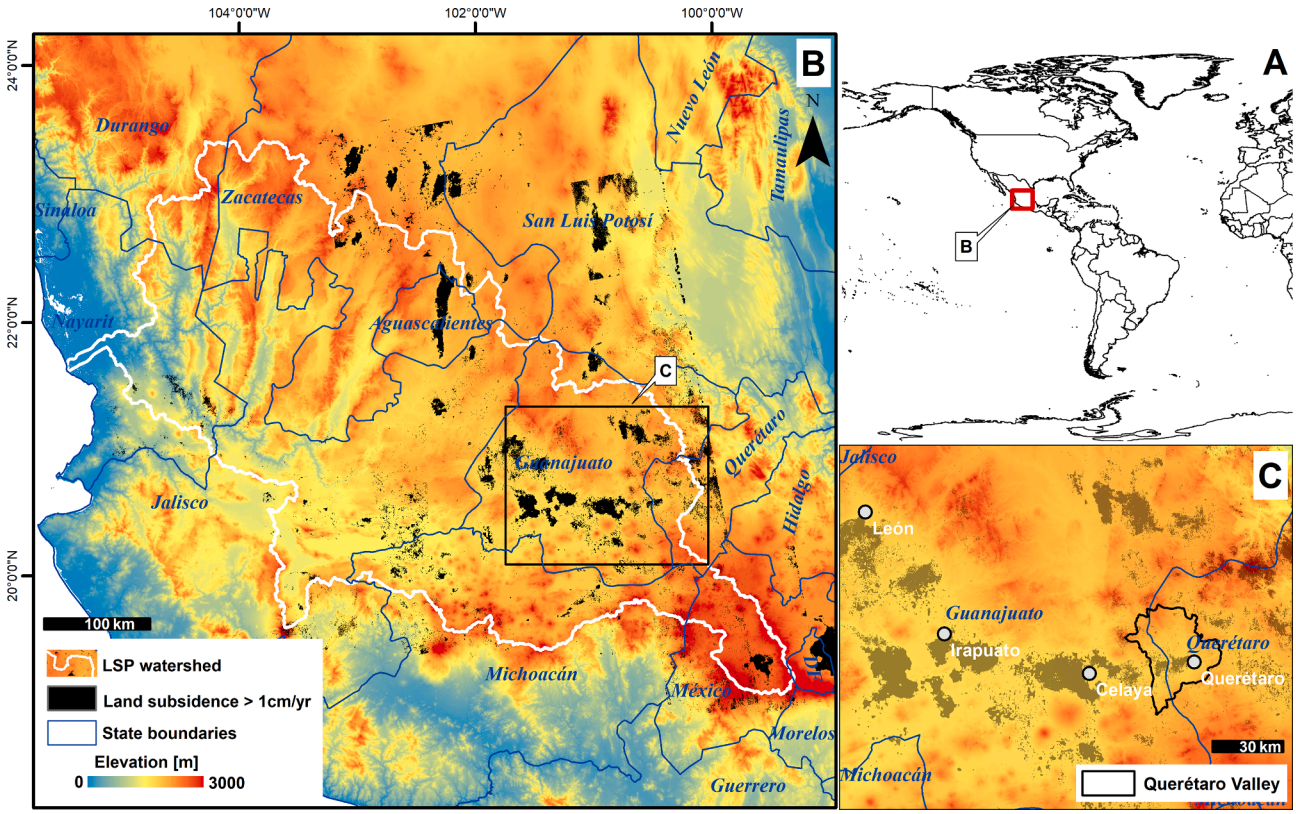

Fig. 1. Location of the study area on global (A), regional (B) and local (C) maps. Areas where land subsidence above 1 cm/yr occurred over 2007–2011 are shown (Chaussard et al. 2014; Castellazzi et al. 2018). The Lerma-Santiago-Pacifico basin is the main water basin of the region (B). The Querétaro-Celaya-Irapuato corridor faces important groundwater depletion-related land subsidence issues (C).

2012; Castellazzi et al., 2016; Suárez et al., 2018) and Ciudad Guzman (Brunori et al., 2015). Encompassing most of these cities, Chaussard et al. (2014) presents a large-scale ground subsidence map for the entire region and for the period 2007–2010, which was later extended northward in Castellazzi et al. (2018). Typically, these subsidence hotspots occur when groundwater is extracted from alluvial and lacustrine aquifers comprising clayey aquitards and interbeds. In some cases, discontinuous volcanogenic sediments occur in between lacustrine and alluvial layers (e.g. Mexico City, Toluca). In other cases, the sedimentary aquifer is within a graben structure controlling its thickness and the ground fracturing observed at the surface (e.g. Celaya, Querétaro, Aguascalientes; see e.g. Pacheco-Martínez et al., 2015a).

Interferometric Synthetic Aperture Radar (InSAR) techniques have largely contributed to map, quantify, and understand groundwater-related land subsidence issues (Galloway and Hoffmann, 2007). It has been applied over numerous cities across Central Mexico, some examples among many others include Cigna et al. (2012), Chaussard et al. (2014), Sowter et al. (2016), Castellazzi et al. (2017). InSAR uses time-series of spaceborne radar images taken from similar orbital positions and analyses the temporal changes of the phase signal. Phase shift maps, also called interferograms, are generated and interpreted as a combination of different contributing signals, such as atmospheric delay, topographic phase (related to spatial baseline and parallax issue due to subtle change in satellite positioning and related inaccuracies), and ground deformation. After correction (for topographic phase removal), stacking and filtering (a frequent strategy adopted for atmospheric phase removal), the residual phase shift can be interpreted as a distance change between the satellite position and the ground. Numerous InSAR processing strategies have been developed in the last two decades. Typically, they either focus on (1) producing many interferograms from a SAR image time-series and fit a deformation model to the interferogram stack (Small BAseline Subset, or SBAS-InSAR; Berardino et al., 2002), or (2) track the phase shifts over the most coherent ground targets (Persistent Scatterers Interferometry, or PSI; Ferretti et al., 2001). While both techniques have their respective advantages, numerous variants attempt to combine the advantages of both (Crosetto et al., 2016). In Central Mexico, both techniques have been applied and show similar results (Castellazzi et al., 2017). In that region, the deformation signals are significant (cm-scale), progressive in both time/ space and occur usually over highly coherent, urban land use. Thus, they are typically easy to retrieve using InSAR.

Aquifer overexploitation and ground fissuring occur throughout Central Mexico; mitigation measures focus on regulatory aspects of groundwater extraction. Typically, groundwater extraction permits are unobtainable or limited in depleting aquifers, which in theory, prevent worsening of the groundwater depletion and ground fissuring issues (Moreno et al., 2010; Hatch Kuri, 2017). However, due to constraint in controlling the extraction rates of authorized users and the constantly increasing demand for water, groundwater extraction is, in most cases, still constantly increasing (Carrera-Hernández et al., 2016). As a result, groundwater depletion, aquifer compaction and ground fissuring still occur despite important consequences on the environment (Esteller and Diaz-Delgado, 2002; Rudolph et al., 2006; Hancox et al., 2010).

A major water importation infrastructure has been inaugurated in 2011: the 'Acueducto II'. This 123-km water pipeline system allows importing water to the city of Querétaro from a nearby mountain range. For the first time in Central Mexico, imported water allows reducing local groundwater extraction, depletion and related ground fracturing issues, meanwhile providing sufficient water for the local populations and the economic development of the region (CEA Querétaro, 2016). While forecasting scenarios of groundwater level recovery have been tested in a three-dimensional groundwater flow modelling effort (Carrera-Hernández et al., 2016), no direct assessment of level recovery and subsidence has been published to date. In this paper, we fill this science

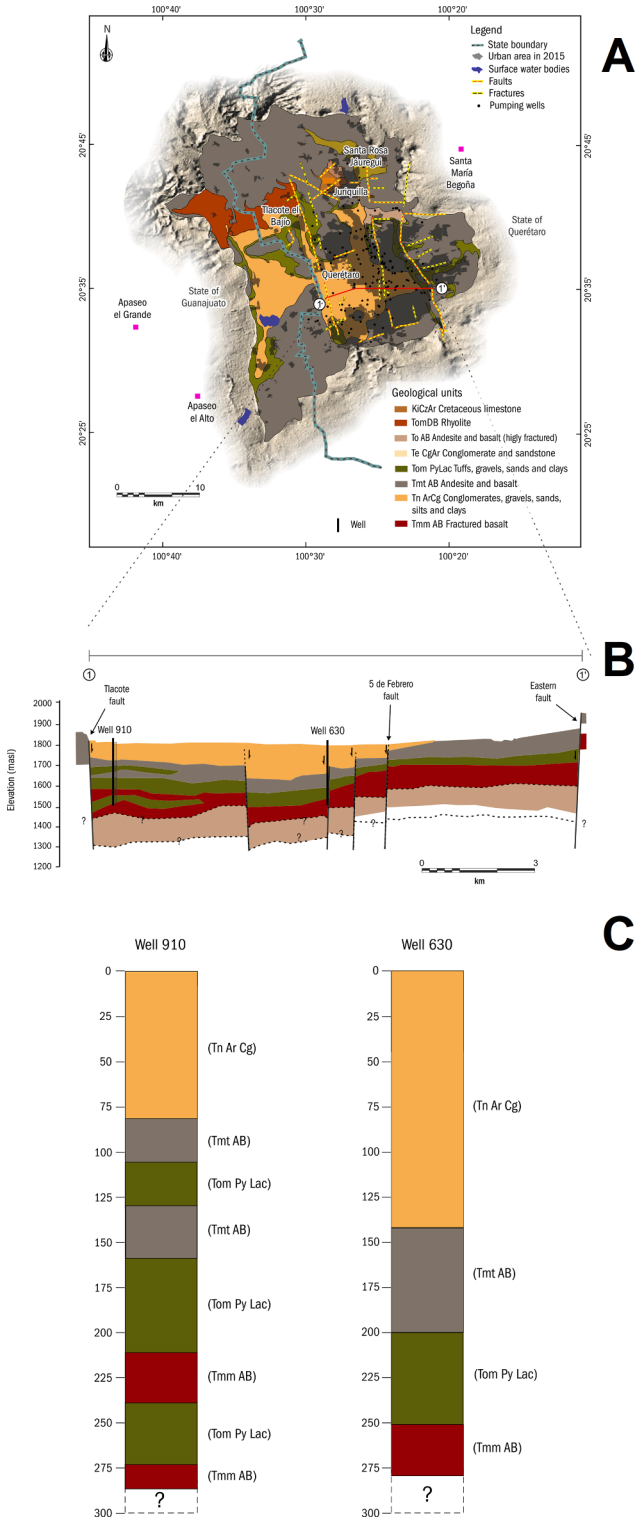

Fig. 2. Geological map of the Querétaro Valley, with extent of the urban area and location of the groundwater extraction wells (A). A geological, conceptual cross-section (B) and two vertical lithological recordings (C) are also presented. Cross section (B) is modified from Carreón-Freyre et al. (2005).

gap by producing a 16-year-long ground deformation time-series from InSAR which encompass the time-period of the water management changes. The interpretation of the deformation time-series is supported by groundwater level measurements and in situ observations.

2. Study area

The City of Querétaro (lat/lon: 21.12/-101.68) lies within the Querétaro Valley, a 2,700 km^2 valley in Central Mexico. It is approximately 200 km northwest of Mexico's capital City, Mexico City (Fig. 1). The valley's elevation is ~1800 m asl and is delimited by mountains to the Northwest and Northeast with elevations in the range [2100, 3400] m asl. The City of Querétaro is the main city within the valley, with a total population (metropolitan area of Querétaro) of 1,161,458 inhabitants in 2010 (INEGI, 2011) and 1,594,212 inhabitants in 2020 (INEGI, 2021), i.e. it increased by +37% in 10 years. The urban area of the Querétaro Valley expanded from 10.65 km^2 in 1973 to 207.33 km^2 in 2015. This is an average spatial expansion rate of 4.7 km^2/yr related to the economic and industrial development within the valley (for more information, see Fig. S1 in the Supplementary info. document).

Geologically, the Querétaro Valley is part of the Trans-Mexican Volcanic Belt (TMVB). The valley is formed by a graben, where lies a sedimentary aquifer. The sediment (and aquifer) thickness is largely controlled by another, smaller-scale graben (Aguirre-Díaz et al., 2005). As other valleys of the region, the sedimentary filling, source of most of the local groundwater extraction, is interrupted sequences of volcanoclastic material, tuffs, and andesitic and basaltic flows of the Pliocene (Fig. 2). Hydrologically, the valley is part of the Lerma-Santiago-Pacifico watershed (Fig. 1) and is connected to the Lake Chapala system, mostly through a relatively limited surface water flow. Average precipitation is ~550 mm/yr and average temperature is ~18.7 degrees Celsius (Villa Alvarado et al., 2014).

The regional hydrogeological setting, as described in Ochoa-González et al. (2018) and Carrera-Hernández et al. (2016), is a cretaceous basement covered by a sequence of alternating layers of tertiary volcanic rocks and sedimentary material. According to the stratigraphic sequence of some wells, a normally graded sedimentary sequence of conglomerates, gravels, sands, silts and clays fills the central area of the valley (Fig. 2). Based on the geologic units of the Querétaro aquifer, the conceptual model has been defined as a multilayer, faulted, unconfined and semiconfined system, as similarly mentioned by Carreón-Freyre et al. (2005, 2016), and more recently by Ochoa-González et al. (2018). Regional groundwater flow, for the most part of the Basin, is controlled by hydraulic head differences and lithology. The main recharge area for the aquifer is in the mountains to the north and south of the valley, and in the Cañada area (east of the city of Querétaro). Local and intermediate groundwater flow systems occur within the aquifer system and a regional flow system occurs through the major faults systems, which may have horizontal and vertical components, frequently related to hydrothermal flows associated with the recent volcanic activity reported in the area (Aguirre-Díaz and López-Martínez, 2001; Ochoa-González et al., 2015). Carreón-Freyre et al. (2005) proposed that the north-south and east-west faulting systems delimit compartments for local and intermediate groundwater flow systems based on the analysis of piezometric level variations. Analysis of piezometric levels allows inferring a direction of groundwater flow from the NE and the NW towards the center of the Querétaro Valley and towards the Apaseo Valley in the state of Guanajuato (west of Querétaro), due to the continuity of the aquifer units.

The local groundwater extraction has increased five folds from 1970 to 2010, with extraction volumes going from 21.0 Mm^3/yr to 61.8 Mm^3/yr. This leads to ever-worsening groundwater level drawdowns and depletion, at least until the potentially drastic changes related to the start of the 'Acueducto II' system in 2011 (CEA, 2016; Carrera-Hernández et al., 2016). According to Pacheco et al. (2006), maximum values of water-table drawdown rates ranged between [4, 6.6] m/yr, with numerous wells showing drawdown close to 3 m/yr. According to Carreón-Freyre et al. (2005), maximum drops in water table between 1970 and 2002 were approximately 160 m in the central area of the valley. In terms of water balance, 105 Mm^3 (Millions of cubic meters, also abbreviated as MCM in other studies) were extracted from the

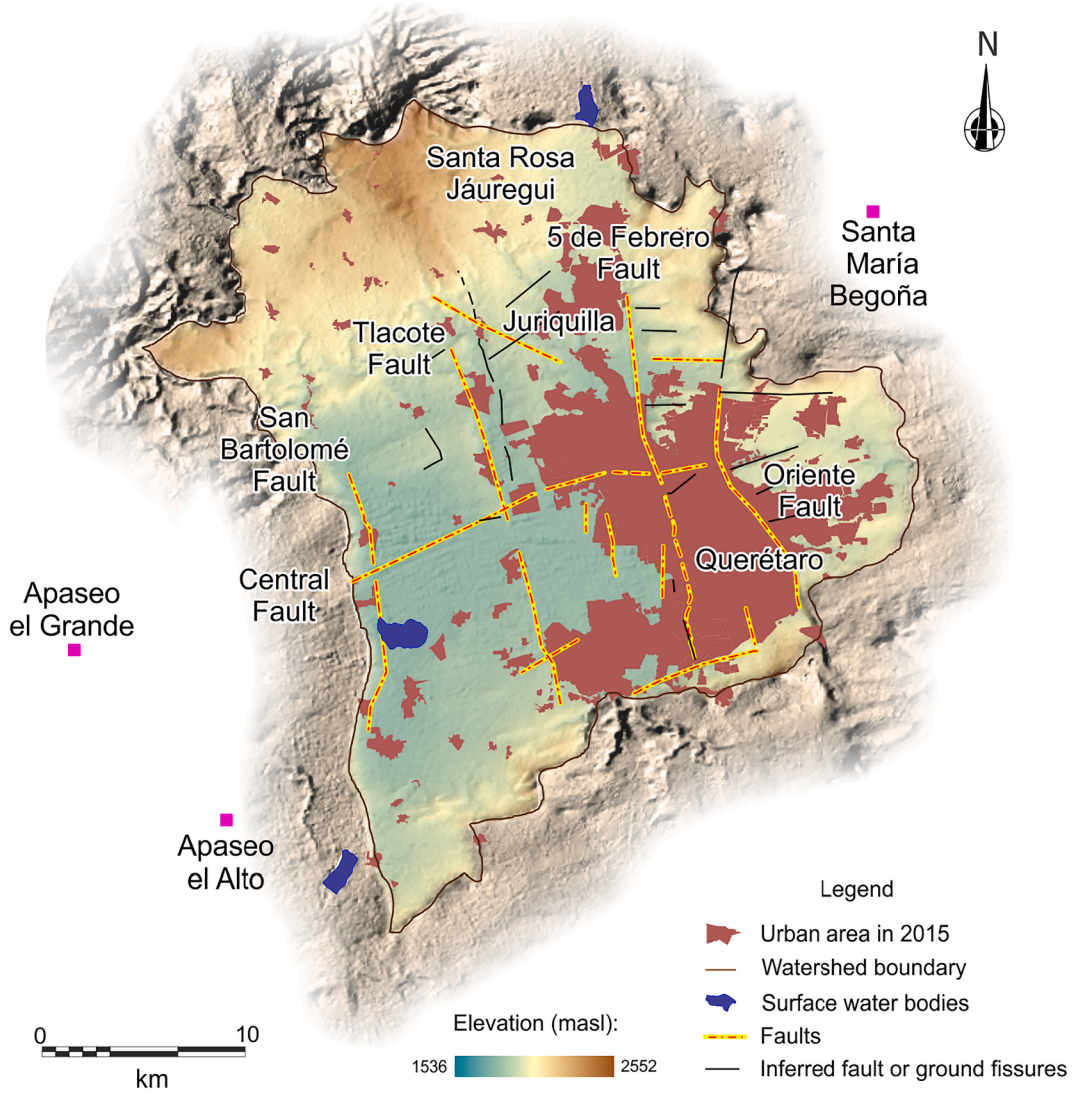

Fig. 3. Ground fracturing in the Querétaro Valley as reported by the State Water Commission of Querétaro (CEA, 2011).

Table 1
Details of the SAR imagery used to measure differential ground displacement in the Querétaro Valley from 2003 to 2017. (ASC: Ascending orbital track; DES: Descending orbital track; IMS: Image Mode Single Look Complex; FBS: Fine Beam Single polarization; FBD: Fine Beam Dual; IW: Interferometric Wide; VV: Vertical-Vertical emitting and recording; HH: Horizontal-Horizontal emitting and recording).

Data source	Mode Path Direction Polarization	Start and end of the time series	Number of images/ interferograms	Looks (Rg × Az)	Approx. LOS angle (deg.)	Coherence threshold
InSAR Envisat ASAR	IMS DES VV	2004-01-19 2005-12-19	18/85	1/7	23.2	0.2
Interpolation	Interpolated from 2005-12-19 to 2007-01-30 using the mean of the two vertical velocities calculated from (1) the last year of the previous time-series and (2) the first year of the subsequent time-series					
InSAR ALOS	FBS/FBD ASC HH	2007-01-30 2010-11-10	15/64	4/9	38.7	0.3
Interpolation	Interpolated from 2010-11-10 to 2011-02 using the mean vertical velocity of the last year of the previous time-series and from 2011-02 to 2013-01-03 using the mean vertical velocity of the first year of the subsequent time-series.					
InSAR Radarsat-2	Ultrafine ASC HH	2013-01-03 2014-11-06	11/49	16/14	47.8	0.2
Interpolation	Interpolated from 2014-11-06 to 2016-10-09 using the mean of the two vertical velocities calculated from (1) the last year of the previous time-series and (2) the first year of the subsequent time-series					
InSAR Sentinel-1A	IW DES VV	2016-10-09 2020-03-22	98/426	4/1	41.7	0.3

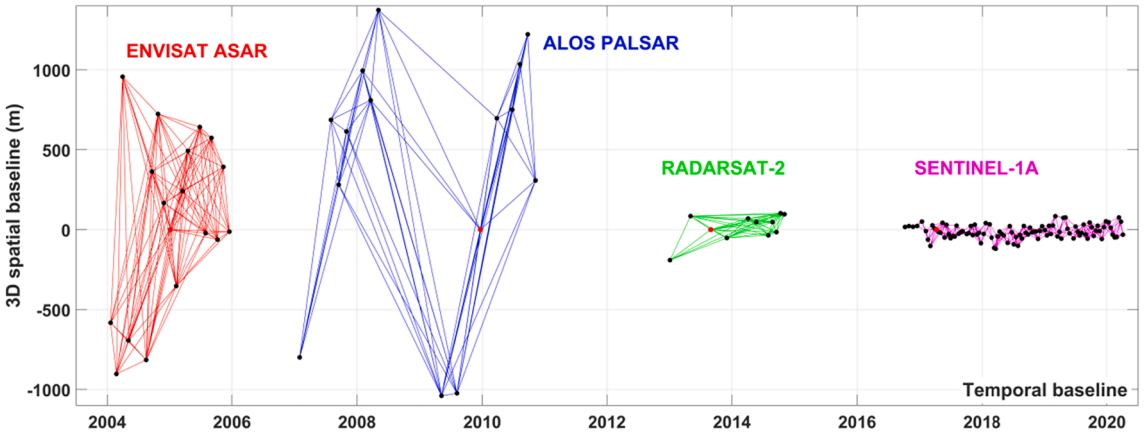

Fig. 4. Combined connection graph for the four SAR time-series processed using SBAS-InSAR. Spatial baselines of SAR acquisitions are in reference to the master image (red dot), all lines represent an interferogram. Note the decrease in spatial baselines with recent SAR sensors, helping with several processing steps such as coregistration of image pairs and topographic phase corrections.

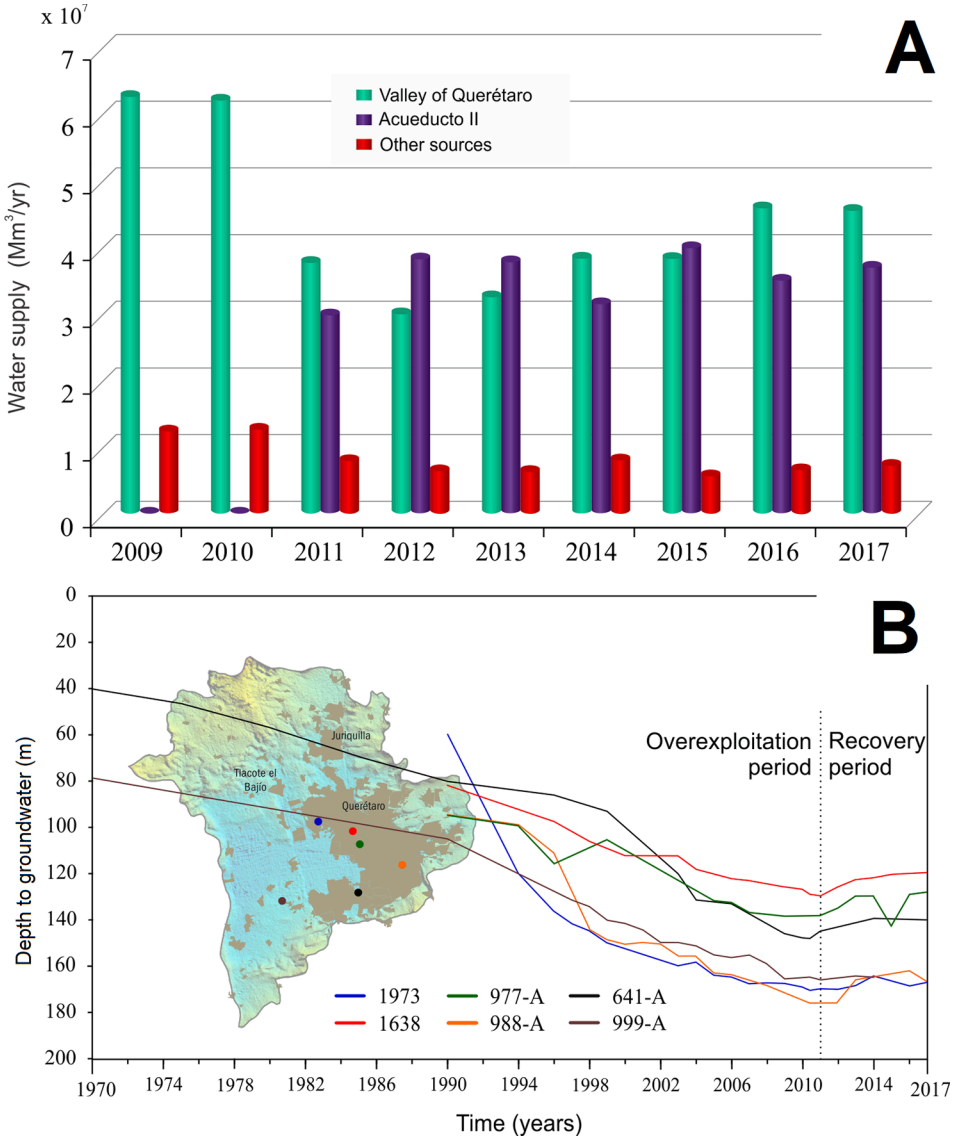

Fig. 5. Sources of water supply in the Querétaro Valley from 2009 to 2017 (A; CEA, 2017). 'Other source' refers to importation from nearby locations such as Amazcala, Huimipan and San Juan del Río. Groundwater level fluctuations at six monitoring wells in the Querétaro Valley Aquifer over two different periods: overexploitation period in 1970–2011 and recovery period in 2011–2017 (B).

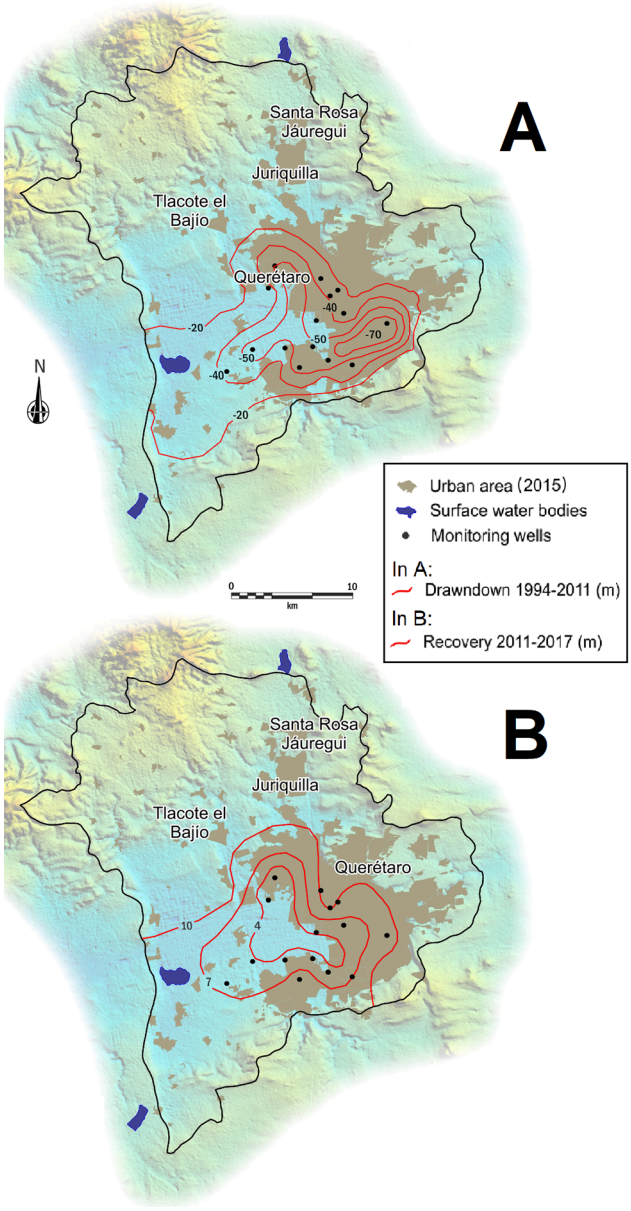

Fig. 6. Water table drawdown in the Querétaro Valley aquifer from 1994 to 2011 attributed to groundwater overexploitation (A), Recovery of groundwater levels in the Querétaro Valley aquifer from 2011 to 2017 (B).

aquifer in 2002 through 304 active pumping wells. Based on the public registry of water rights (REPDA), there were 469 active extraction wells in the Querétaro Valley, among which 313 are in the state of Querétaro and 156 in the state of Guanajuato (Fig. 2). The 'Acueducto II' water importation system has allowed reducing the local groundwater extraction, and its consequences on groundwater levels has been modelled by Carrera-Hernández et al. (2016), who projected a short-term recovery of groundwater levels followed by depletion, with groundwater levels reaching again 2010′s levels in 2020 and decreasing further from there.

Ground fracturing has been studied in Querétaro (Pacheco et al., 2006; CEA, 2011; Ochoa-González et al., 2014) and a series of ground fractures have been identified (Fig. 3). As for other cities of the area facing regional-scale groundwater depletion, the sediment thickness and compressibility are the major controls for spatial patterns and amplitude of land subsidence (Fig. 2C). The underlying fault system has controlled the deposition of volcanogenic and lacustrine sediments during the geological history of the valleys, leading to largely uneven thickness of compressible sediment layers. This leads to a varying sensitivity to poro-elastic compaction when integrated over the total thickness of the aquifer (1D-integrated). Uneven land subsidence creates ground rupture lines, or fractures, often aligned with the topography of the hard rock basement and major faults systems. In Querétaro Valley, this has been confirmed by Carreon-Freyre and Cerca, (2006) who used Ground Penetrating Radar to map buried faults. They concluded that the major ground fracture (the '5 de Febrero' fracture) is aligned with a buried fault scarp. Differential deformation has been studied in Pacheco et al. (2006) and in several studies using InSAR (Farina et al., 2008; Chaussard et al., 2014, Castellazzi et al., 2016). According to these studies, vertical deformations in the range [−80, −30] mm/yr occur. They all report steep spatial gradients of deformation and ground fracturing due to discontinuous compressible sediment layers, spatially controlled by buried faults and grabens and typical in the cities of the region.

3. Materials and methods

3.1. Monitoring ground deformations with InSAR

To retrieve the subsidence rates that occurred before and after the change in water management, the Interferometric Synthetic Aperture Radar (InSAR) technique was applied over four SAR imagery time-series from Envisat, ALOS-1, Radarsat-2, and Sentinel-1A. The four time-series encompass the period 2004–2020 with few temporal gaps: ~13 months between 2010-11-10 and 2013-01-03 and ~23 months between 2014-11-06 and 2016-10-09 (Table 1). The InSAR processing follows the Small Baseline Subset Interferometry (SBAS-InSAR) technique developed by Berardino et al. (2002).

InSAR processing was performed with SARSCAPE 5.5.4; the main processing parameters and the connection graphs for each processing are presented in Table 1 and Fig. 4. They were optimized to retrieve displacements at a 30-m spatial resolution, by adjusting the resolution factors (looks) according to the original resolution of each imagery products (Table 1). The topographic phase was extracted from all interferograms using a 30 m resolution Digital Elevation Model derived from optical imagery (ALOS-3D; Takaku et al., 2014). The phase-to-displacement inversion was computed by fitting a linear deformation model to the interferogram stack. A spatio-temporal atmospheric filtering of 500 days (high pass) and 1200 m (low pass) was applied to all time-series but Sentinel-1A, which was filtered with a 365 days filter (high pass). All InSAR processing but Sentinel-1A were optimized to retrieve mean velocities over their respective observation periods, with the potential tradeoff that seasonal variation of deformation signals might be interpreted as atmosphere delay and extracted during the SBAS inversion procedure. The four SAR time-series were acquired with different Line-Of-Sight (LOS) angle. As aquifer compaction mainly implies vertical deformation, all InSAR-derived LOS deformation time-series were converted to vertical displacements assuming the horizontal displacement negligible (Castellazzi et al., 2016, 2017; Chaussard et al., 2014). After processing and conversion to vertical deformation, the resulting vertical displacement maps were aggregated into one time-series by filling temporal gaps using the linear interpolation approach detailed in Table 1. Throughout this article, negative deformation rates mean ground subsidence, positive rates mean ground uplift.

3.2. Auxiliary datasets

The piezometric history of the Querétaro aquifer was developed from well level time-series of 15 monitoring wells provided by the National Water Commission (CONAGUA). This dataset allowed tracking the evolution of the water-levels from 1970 to 2017. The water-level data from the monitoring wells were converted from depth-below-surface data to water-table-elevation data (meters above sea level). These data were then projected on a map of the Querétaro Valley and lines of water

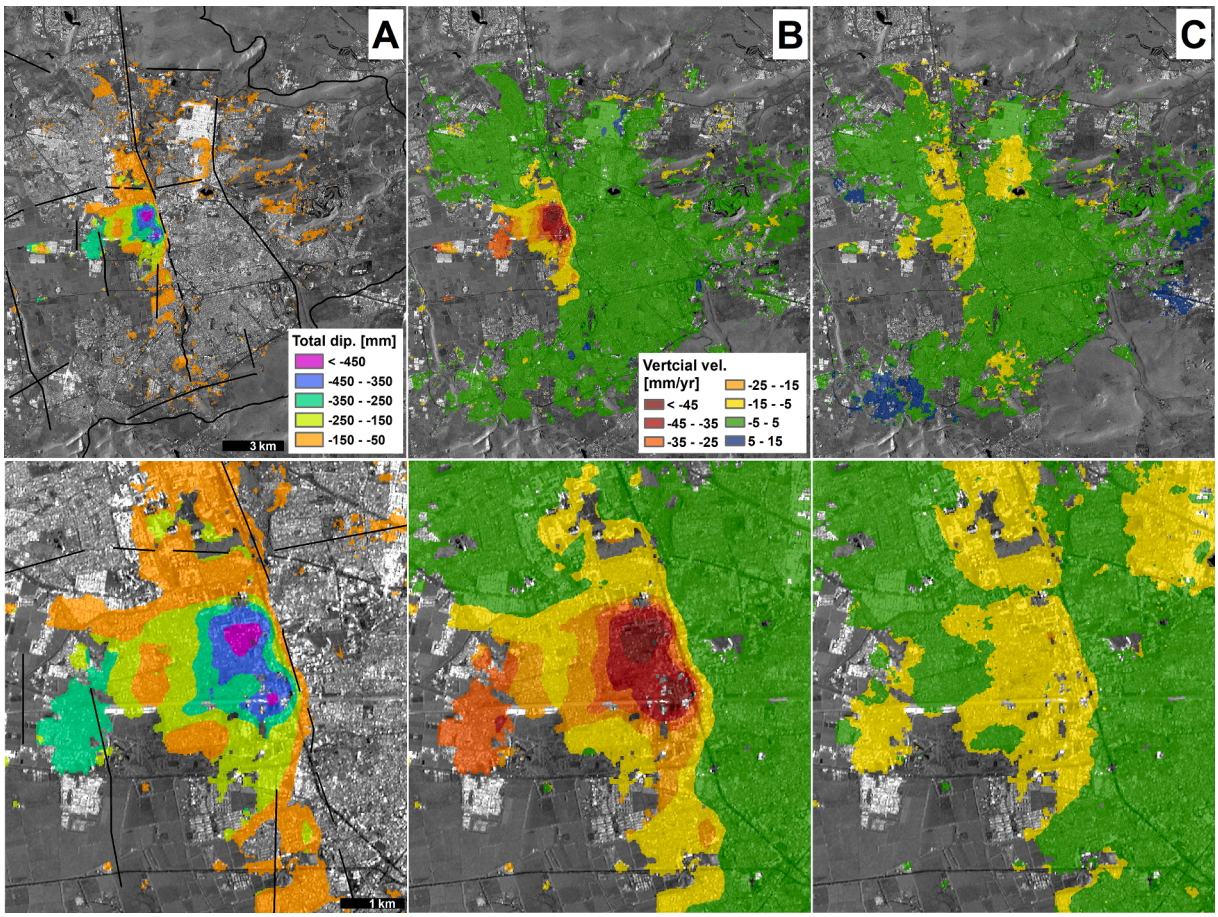

Fig. 7. Total InSAR-derived vertical ground displacement from 2006/02 to 2020/03 (A); Vertical displacement velocity before (B) and after (C) 2011/02. Below each figure, a zoomed view over the '5 de Febrero' fracture (differential deformation) is shown.

table drawdown were drawn from 1994 to 2011 (overexploitation period) and from 2011 to 2017 (recovery period). The interpolation between the observation points at the monitoring wells required to produce continuous potentiometric groundwater level maps is based on a kriging approach.

4. Results and discussion

4.1. Groundwater level response to the water management change

The long-term evolution of water sources for the City of Querétaro is presented in Fig. 5A. The water management shift of 2011 is obvious, and local groundwater extraction was cut by half and compensated by water imports from the 'Acueducto II' system. While the water imports from the Acueducto II system have fluctuated in the range [2.9, 3.9] 10^7 Mm^3/yr, the local groundwater extraction has been in constant increase since 2012, one year after the implementation of the water import system. The graph (Fig. 5A) shows that the import system has allowed a drastic decrease in local extraction. It also shows that the increasing water demand is fulfilled through increased pressure on existing groundwater extraction infrastructure.

Groundwater level curves are presented in Fig. 5B and piezometric level changes are presented in Fig. 6. We note the fast decline of groundwater levels occurring in the Querétaro Valley prior to 2011 (Fig. 5B and 6A). Some wells are showing a total groundwater level decrease of 100 m during the 1970–2010 era, with up to 70 m of piezometric level drawdown during the 1994–2011 era (Fig. 6A). An average groundwater decrease rate of 2.5 m/year is measured, which agrees with observation from Pacheco et al. (2006).

The implementation of the water import scheme marks an important breaking point in all groundwater levels curves. A level recovery is observed in the subsequent years (Fig. 6B). Most of the wells impacted by this decrease in extraction rates are located at the margin and not in the centre of the drawdown area, allowing the important recovery of the groundwater hydraulic head in the Northern and North-eastern part of the city. We note, however, that for four of the six water level curves presented, the recovery is significantly slower than the groundwater depletion observed prior to 2011 (Fig. 5B). This suggests that, without accounting for the non-linearity of the water level reaction, the related changes in discharge/recharge fluxes (Bredehoeft, 2002) and assuming groundwater extraction as stable in the future (which is not supported by Fig. 5A), the recovery processes should be occurring for a longer period than the depletion has already occurred (at least 40 years).

4.2. Ground level response to the water management change

Fig. 7 presents a summary of the InSAR results, including the total subsidence for the entire study period (Fig. 7A), the mean vertical velocity prior to (Fig. 7B) and after (Fig. 7C) the water management change. Figs. S2 and S3 (Supplementary info.) present the InSAR-derived ground deformation rates and the precision of the InSAR observations separately for each sensor. As significant changes in groundwater levels are observed, significant changes in land subsidence amplitude and spatial patterns are expected. It is important to keep in mind that the two phenomena are not synchronous, and a time delay is expected. For example, Calderhead et al. (2011) analysed extensometer data and observed a 4–5 months delay between groundwater drawdowns and compaction in the Toluca Valley. The same study considers

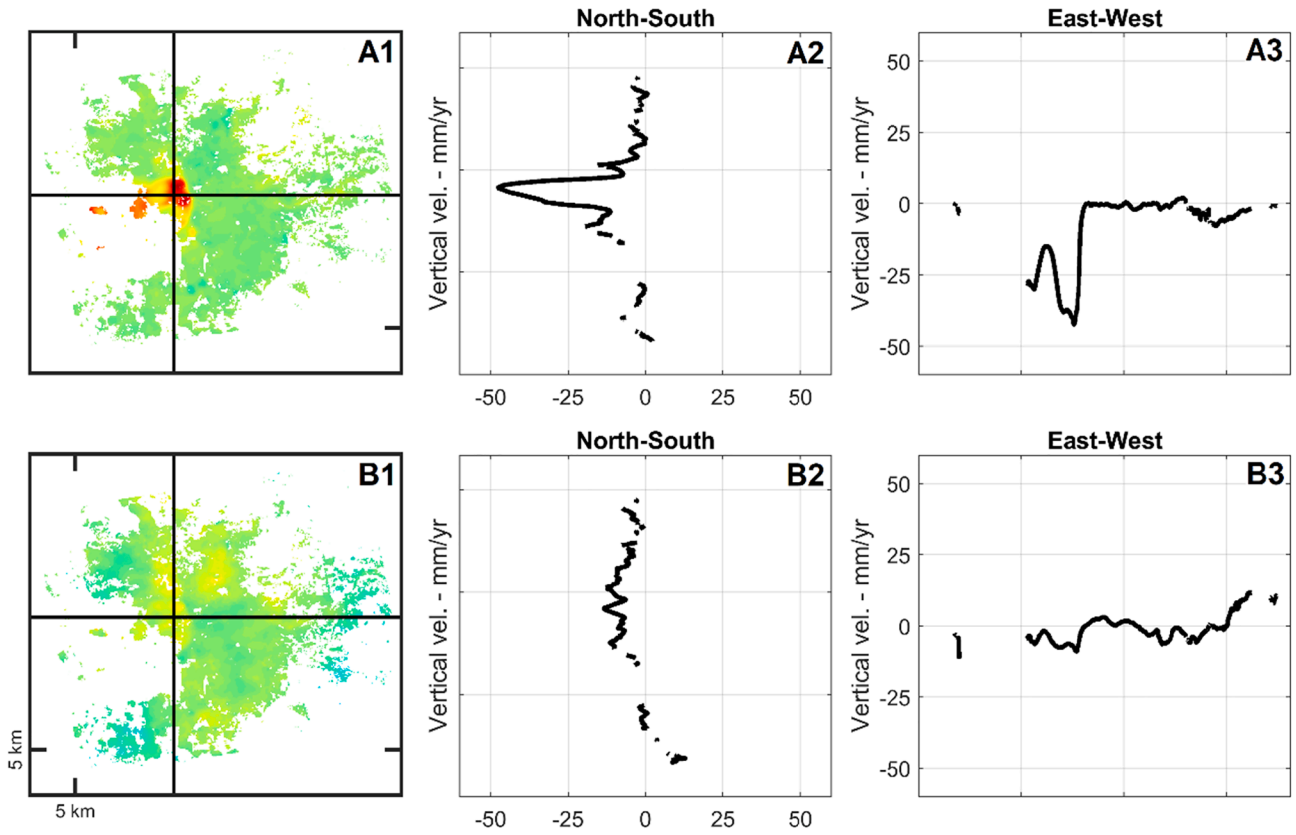

Fig. 8. North-South and East-West transects of mean ground deformation before (A1-A2-A3) and after (B1-B2-B3) the water management shift of 2011/02. Note that A2 vertically aligns with A1, and B2 vertically aligns with B2.

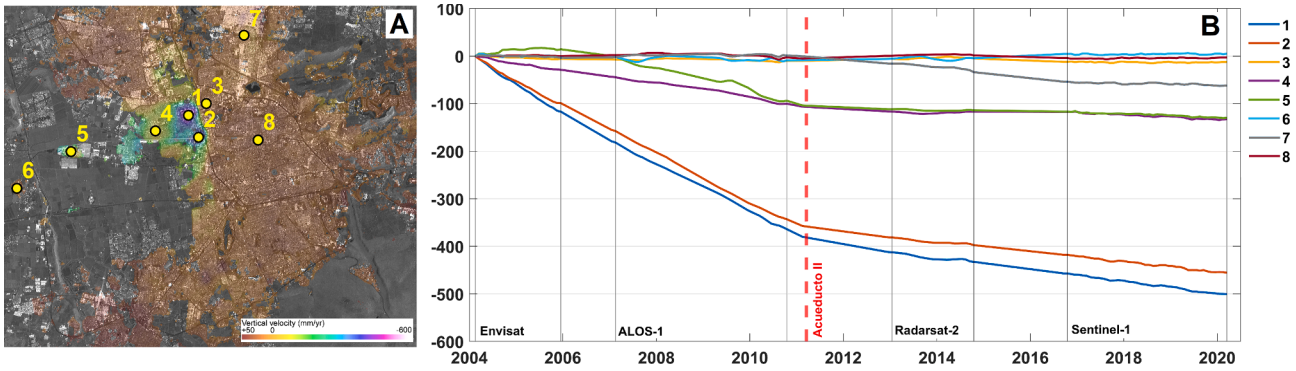

Fig. 9. 16 years of ground displacements in eight selected locations in and around the City of Querétaro (A: locations, B: ground deformation time-series). Time windows corresponding to the four InSAR time-series and start of the Acueducto II system are overlaid on the graph (B).

that as a relatively rapid reaction compared to e.g. Mexico City. No estimation of the time delay is available for the Querétaro Valley to this date.

While most of the city is stable, with total InSAR deformation in the range [-50, 50] mm in 16 years (Fig. 7A). This coincides with an acceptable InSAR measurement noise level of approximately [−3, 3] mm/yr, which is typical for SBAS-InSAR in such favorable, highly coherent, urban settings (Fig. S3). A major land subsidence feature is observed west of the '5 de frebrero' fracture, which generates the differential ground deformation and the constant fissuring along that fracture. This subsidence pattern coincides with an important increase in the thickness of the sedimentary and volcanoclastic filling as shown in Fig. 2B/C. Most of the area west of the fracture shows total subsidence in the range [−180, 300] mm, with a limited area subsiding up to −550 mm in its center. The subsidence area extends westward in a U-shape pattern, with the highest rates close to the fracture line.

Mean deformation rates prior to the 2011 water management change are presented on Fig. 7B and Fig. 8A, where similar patterns to Fig. 7A can be observed. The mean vertical velocity west of the '5 de Febrero' fracture is in the range [−50, −30] mm/yr. This is slightly less than the subsidence rates of [−80, −50] mm/yr measured for 2003–2005 by Farina et al. (2008), who used Differential-InSAR (single interferogram) and Envisat imagery. However, it is in good agreement with Chaussard et al., (2014), who studied the period 2007–2010 with ALOS and measured deformation in the range [−50, −30] mm/yr (see Fig. S2 for results of individual InSAR time-series). The results prior to 2011 presented here (Fig. 7B) are based on the same radar imagery as Chaussard et al. (2014), but also integers significantly longer Envisat observations to covers the time-period 2004–2006.

InSAR results for the period post-2011 are based on processing

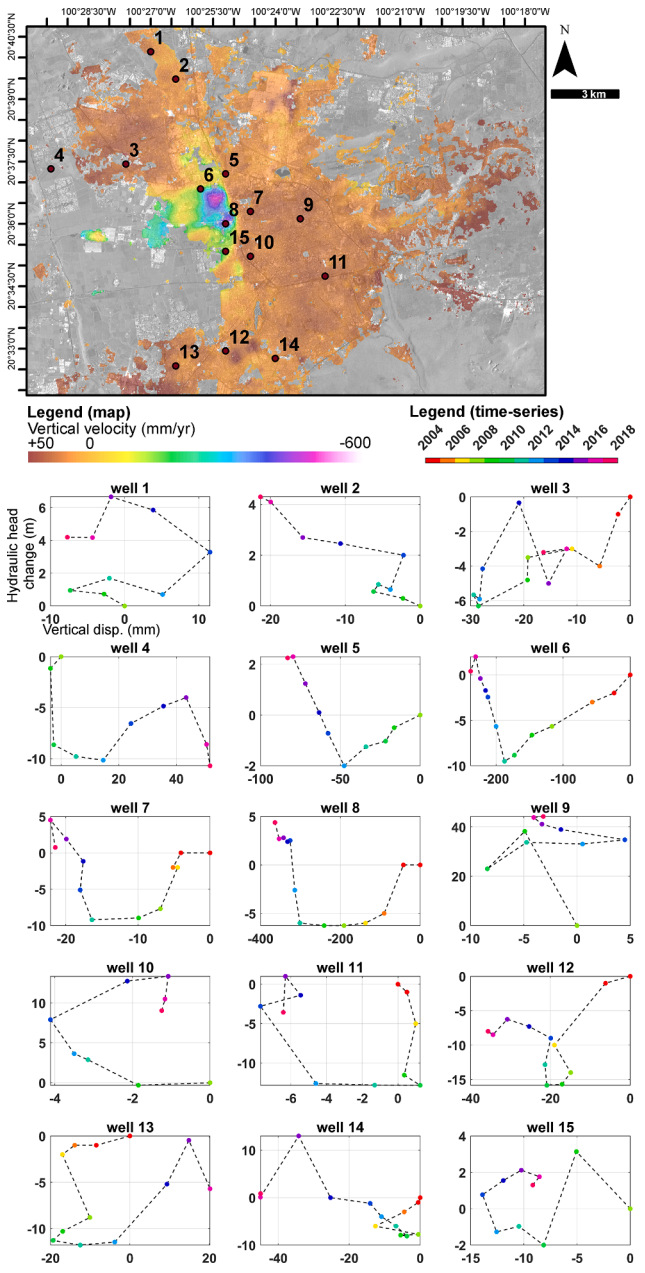

Fig. 10. Yearly changes in hydraulic pressure in the aquifer (in m; Y axis) compared with yearly changes in ground level (in mm; X axis) at 15 locations. Both data are expressed in terms of change (starting at 0) from the first groundwater pressure measurement.

Radarsat-2 and Sentinel-1 imagery products. The mean absolute vertical velocity is significantly lower than prior to 2011 (Fig. 7C, Fig. 8, Fig. S2C/D). The subsidence area west of the '5 de Febrero' fracture is still visible, but the signal amplitude is greatly reduced to [−5, −12] mm/yr of vertical velocity. These rates are still relatively low but still beyond a typical SBAS-InSAR detection threshold (Fig. S3C/D). This suggests that low rates of subsidence still occur post-2011 and that the fissuring along the '5 de Febrero' fracture is still active. Another low-amplitude, spatially progressive subsidence patch is also observed North of the City. This anomaly was not observed during any InSAR survey for the period prior 2011 (Fig. S2C) and is only observed in the Radarsat-2 deformation time-series (2013-01 to 2014-11; Fig. 2C). There is, to this date, no explanation for the presence of this subsidence feature. Small-scale uplift signal beyond detection threshold is also detected (Fig. 8B2; 8B3, S2).

The temporal evolution of land subsidence rates is presented in Fig. 9, where deformation time-series are drawn for 7 selected pixels across the InSAR coverage. Points 3 and 5 are located east of the '5 de Febrero' fracture and in the city center, respectively. They show similar InSAR signal without any apparent deformation anomaly. Point 7 is west of the city, far from the '5 de Febrero' deformation area and is also stable. Point 4 and 6, located west of the '5 de Febrero' fracture, are representative of medium subsidence rates for that area, with ~−15 mm/yr prior to 2011, and ~−5 mm/yr post-2011. Points 1 and 2, located in the area with the highest subsidence rates, west of the '5 de Febrero' fracture, show subsidence rates of −50 mm/yr prior to 2011, and mean rates in the range [−8, −10] mm/yr after 2011.

Fig. 10 compares yearly, vertical ground deformation values and yearly averaged depth to groundwater levels. It allows observing the ground level reaction to groundwater level stabilization and/or recovery after the 2011 water management change. The graphs start at 0 for both data at the first year for which both measurements are available, and every subsequent point corresponds to a subsequent year. Due to the challenges of interpreting groundwater heads in individual wells (lithological heterogeneity and varying degrees of connectivity to the regional aquifer for each well and accuracy of the level measurements), we provide a general interpretation, but we do not discuss the head/deformation relationship specifically for each well. First, we note that, as observed previously, groundwater levels have increased after 2011. We observe level recovery in the range [5, 15] m in the four years following the management change in most wells. Second, we confirm that the breaking points for most graphs corresponds to 2010–2011, when the groundwater management change occurred. Levels in wells 10 and 12 have started to rise earlier that 2010, suggesting that other local controls on groundwater levels occur for some wells, e.g. extraction have stopped in a nearby well. Third, we observe that for some wells (6, 7, 8 and 11), the ground level stabilized while the groundwater level recovered. For other wells (3, 10, 13, 15), a slight uplift is detected while groundwater levels increase. Fourth, we note that, after a recovery in 2011–2015, groundwater level started to decline again during the period 2015–2017 for most wells (1, 3, 6, 7, 10, 11 and 15). This analysis highlights the spatially varying nature of the reaction between groundwater pressure and ground levels, and a varying portion of elastic vs. inelastic deformation. As expected for this region, the reaction can be considered as largely inelastic. This is confirmed by the deformation behavior at well 6, where the most subsidence occurred prior to 2011, which does not show any major elastic uplift signal after 2011. In addition, the InSAR measurement can be considered as being accurate around that well: it is where the InSAR signal-to-noise ratio is the most favorable. Contrastingly, the analysis over wells with small deformation rates (e.g. 10 and 11) might be influenced by InSAR noise (Fig. S3).

4.3. *Recent ground deformation in Querétaro*

This section analyses solely the InSAR results produced with Sentinel-1 and representative of the most recent period: 2016-10 to 2020-03 (Fig. 11, with corresponding precision estimates presented in Fig. S3D). Sentinel-1A, with its repeat path frequency of 12 days and its relatively short spatial baselines (Fig. 4) provides adequate InSAR precision to analyze the small amplitude deformations occurring in Querétaro over the recent years (2017–2020). While groundwater level observations were not available for that study period, the increasing groundwater extraction trend shown on Fig. 5A and the groundwater level decline observed in some wells after 2015 (Fig. 10) might lead again to groundwater extraction beyond sustainable levels, as prior to 2011.

The mean vertical velocity map derived from Sentinel-1A data shows that the major subsidence area corresponding to the differential deformation east of the '5 de febrero' fracture is still active (Fig. 10-a), with rates in the range [-15, −10] mm/yr. We note, however, that the 'bowl' shape of the deformation (Fig. 6A) has changed to a spatially diffuse

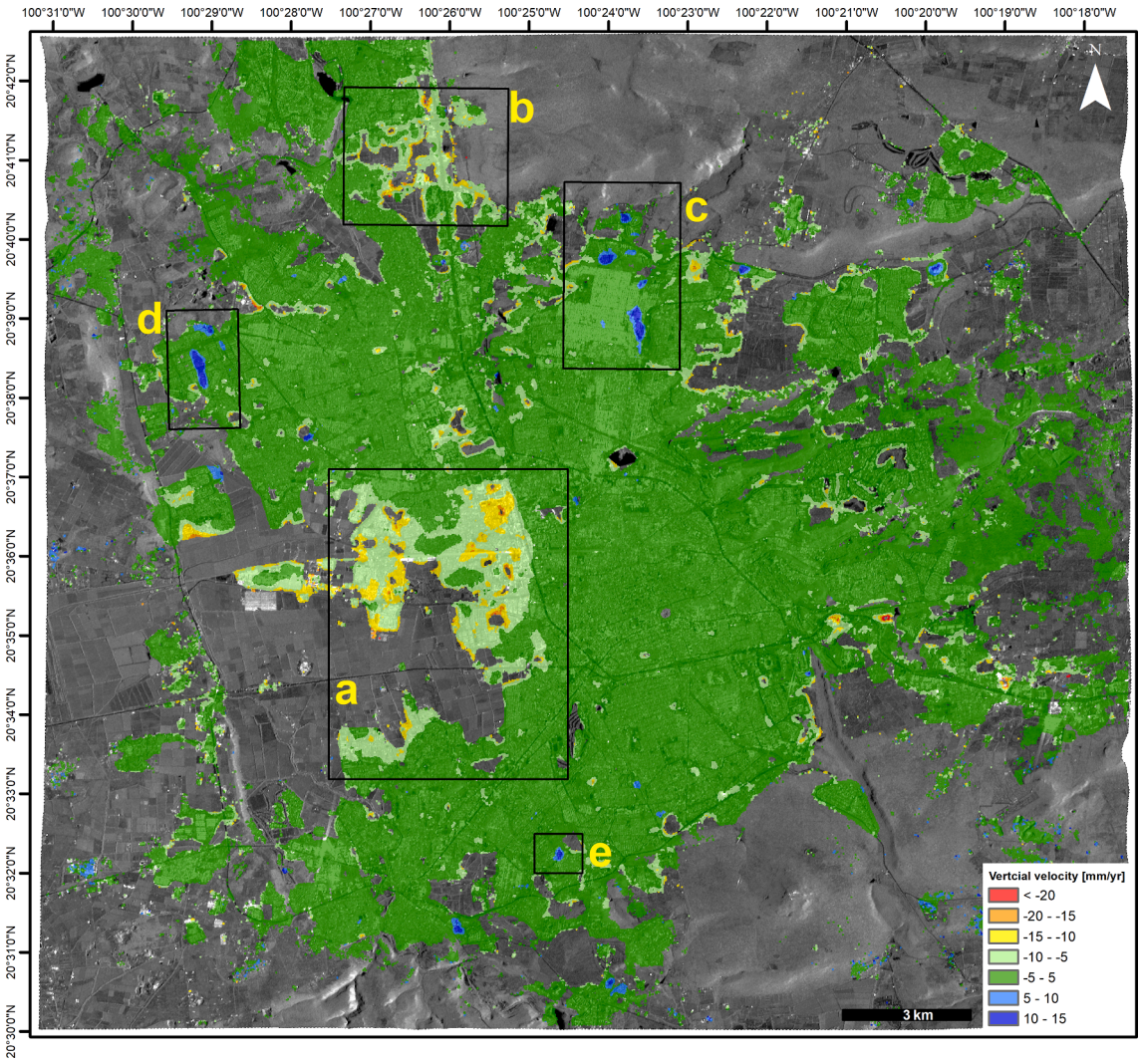

Fig. 11. Mean ground vertical velocity map produced by InSAR and based on 98 Sentinel-1A images acquired between 2016-10-09 and 2020-03-22. The density of Sentinel-1 allows better precision than the three other InSAR processing presented in this study over the same area. The map presents the recent rates of deformation, with notable features highlighted by squares a-b-c-d-e.

deformation signal (Fig. 11). A subsidence area with lower amplitude in the range [-5, −8] mm/yr is also observed north of the city (Fig. 11b). Few localized uplift area in the range [+12, +17] mm/yr are detected (Fig. 11c,d,e). No definitive explanation is available for these localized uplift areas to this date. They seem unlikely related to a potential groundwater level recovery occurring during that time-period, as these small-scale areas were not identified as groundwater-related subsidence hotspots in this paper nor in any previous work. A more likely explanation is provided by Pacheco et al. (2006), who identified localized uplift deformation from expansion of surficial clay lenses after rainy seasons. It is important to note that the diffuse, low amplitude subsidence anomaly west of the '5 de Febrero' subsidence area and present on Fig. 7C does not appear on Fig. 11. Fig. 7C presents a combination of the Radarsat-2 and Sentinel-1 InSAR observations (2013–2020), suggesting that such anomaly is detected solely in the Radarsat-2 InSAR maps (see also Fig. S2C/D). In other words, it occurred in the 2013–2014 period, but not in 2016–2020, highlighting the variable nature of subsidence spatial patterns and rates, as noted earlier. Finally, we note the presence of minor deformation signals at the margin of the urban, coherent areas (e.g. south-east of square c, Fig. 11), which we do not interpret as real ground deformation, but rather as a processing artefact related to a higher level of InSAR noise (Fig. S3D).

Given the usual, monthly-scale, time gap from decline in groundwater levels to compaction/subsidence in the region (Calderhead et al., 2011), residual, time-lagged deformation from past groundwater level decline seems unlikely to be the only reasons for the recent subsidence rates. Thus, the only remaining hypothesis to explain the reactivation of the subsidence is that increasing groundwater extraction (Fig. 5A) observed from 2012 has led to additional groundwater drawdowns beyond critical heads (past minimums). The depletion rate is, however, likely much smaller than prior to 2011. This interpretation is supported by the results shown on Fig. 11 and by the decadal time-series presented on Fig. 9 (Points 1 and 2): the subsidence rates observed by Sentinel-1 in 2017–2020 are slightly more important than the ones observed by Radarsat-2 (2013–2014). This suggests that the 2011 groundwater management change has been efficient to reduce the important groundwater depletion, important subsidence rates and related fracturing in the short-term (2011–2017). The increasing water demand has pushed groundwater extraction to unsustainable levels again over the recent years. Such observation is generally consistent with groundwater budget forecasting provided by scenario 1 in Carrera-Hernández et al. (2016), who suggested that the implementation of the 'Acueducto II' system will only decrease and delay the groundwater depletion issue. They estimated a short-term recovery of groundwater levels followed by a decline, with levels of 2010 reached again in 2020. Their simulation, however, assumed the groundwater extraction rates to

be constant after 2011. As groundwater extraction has followed a positive trend since 2011 (see Fig. 5A), the predicted switch between positive to negative aquifer water budget might have occurred slightly earlier than predicted by their simulation, and their forecasting of water levels might have been slightly optimistic (higher than actual).

5. Conclusions

The city of Querétaro faces long-term groundwater depletion issues and prone to medium rates of ground subsidence for the region up to 50 mm/yr. More importantly, the land subsidence patterns are highly heterogenous in space, with a major fracture system with differential deformation going from zero deformation (on one side of the fracture) to maximum rates (on the other side). Typical for the region, this is known to be spatially related to buried fault systems and grabens controlling the compressible sediment thickness. From 2011, a large water importing project was implemented to reduce local groundwater extraction by half and solve the related issues. This paper studies the changes in both groundwater levels and subsidence rates as a result of this project.

Decadal-scale decline of groundwater levels of ~2.5 m/yr were observed prior to 2011. As predicted by groundwater models and level forecasts previously published (Carrera-Hernández et al., 2016), groundwater levels recovered in 2011 due to the reduced extraction rates in the valley. Land subsidence was reduced by a factor of ~5 in the subsequent years (2011–2015), down to a maximum of 10 mm/yr. Few years later, in the period 2015–2017, groundwater levels started to decline again, at significantly smaller rates than prior to 2011. Land subsidence also started to show minor signs of increase during that period, as observed by the Sentinel-1 InSAR time-series covering 2017–2020.

The case of Querétaro is the first large-scale implementation of a major groundwater depletion and subsidence-mitigating project in Central Mexico. Given that all major cities of the region (e.g. Toluca, Morelia, Aguascalientes, Celaya) are facing the same issues, it is particularly interesting to observe how such a drastic change is efficient in solving the issues. We note, however, that the different geographical and hydrological settings of major cities in Central Mexico allow for different solutions, and that the case of Querétaro is not transposable to others. In some cases, the local water sources must be shared with nearby cities, as it is the case in Toluca and Mexico City.

CRediT authorship contribution statement

Pascal Castellazzi: Conceptualization, Methodology, Investigation, Formal analysis, Data curation, Writing – review & editing, Writing – original draft. **Jaime Garfias:** Methodology, Data curation, Investigation, Writing – review & editing, Formal analysis, Supervision, Project administration. **Richard Martel:** Methodology, Writing – review & editing, Supervision, Project administration.

Declaration of Competing Interest

The authors declare that they have no known competing financial interests or personal relationships that could have appeared to influence the work reported in this paper.

Acknowledgments

The authors would like to thank CSIRO's Deep Earth Imaging FSP, the Ministère des Relations internationales Francophonie et Commerce extérieur du Québec (MRIFCE - Québec), the Consejo Nacional de Ciencia y Tecnología (CONACyT - Mexico), and the Natural Sciences and Engineering Research Council of Canada (NSERC - discovery grant of Richard Martel; grant number RGPIN-2016-06503) for their financial supports. We acknowledge Natural Resources Canada (NRCAN) and the Canadian Space Agency (CSA) for their help in obtaining Radarsat-2 acquisitions over Mexico under the MURF #CG0063. We acknowledge the European Space Agency (ESA) for providing Envisat ASAR and Sentinel-1 IW data. We thank the SARMAP team for their help and their efforts in continuously improving the SARScape InSAR processing toolbox.

Appendix A. Supplementary material

Supplementary data to this article can be found online at https://doi.org/10.1016/j.jag.2021.102632.

References

Aguirre-Díaz, G.J., López-Martínez, M., 2001. The Amazcala caldera, Queretaro, Mexico. Geology and geochronology. J. Volcanol. Geotherm. Res. 111 (1-4), 203–218. https://doi.org/10.1016/S0377-0273(01)00227-X.

Aguirre-Díaz, G.J., Nieto-Obregón, J., Zúñiga, F.R., 2005. Seismogenic basin and range and intra-arc normal faulting in the central Mexican Volcanic Belt, Querétaro, México. Geol. J. 40 (2), 215–243. https://doi.org/10.1002/gj.1004.

Berardino, P., Fornaro, G., Lanari, R., Sansosti, E., 2002. A new algorithm for surface deformation monitoring based on small baseline differential SAR interferograms. IEEE Trans. Geosci. Remote Sens. 40 (11), 2375–2383. https://doi.org/10.1109/TGRS.2002.803792.

Biot, M.A., 1941. General theory of three-dimensional consolidation. J. Appl. Phys. 12 (2), 155–164.

Bredehoeft, J.D., 2002. The water budget myth revisited: why hydrogeologists model. Groundwater 40 (4), 340–345.

Brunori, C.A., Bignami, C., Zucca, F., Groppelli, G., Norini, G., Davila Hernández, N., Stramondo, S., 2015. Ground Fracturation in Urban Area: Monitoring of Land Subsidence Controlled by Buried Faults with InSAR Techniques (Ciudad Guzmán: Mexico) BT - Engineering Geology for Society and Territory - Volume 5. In: Lollino, G., Manconi, A., Guzzetti, F., Culshaw, M., Bobrowsky, P., Luino, F. (Eds.), Springer International Publishing, Cham, pp. 1027–1031.

Calderhead, A.I., Martel, A., Alasset, P.-J., Rivera, A., Garfias, J., 2010. Land subsidence induced by groundwater pumping, monitored by D-InSAR and field data in the Toluca Valley, Mexico. Can. J. Remote Sens. 36 (1), 9–23. https://doi.org/10.5589/m10-024.

Calderhead, A.I., Therrien, R., Rivera, A., Martel, R., Garfias, J., 2011. Simulating pumping-induced regional land subsidence with the use of InSAR and field data in the Toluca Valley, Mexico. Adv. Water Resour. 34 (1), 83–97. https://doi.org/10.1016/j.advwatres.2010.09.017.

Carreón-Freyre, D., Cerca, M., Luna-González, L., Gámez-González, F.J., 2005. Influencia de la estratigrafía y estructura geológica en el flujo de agua subterránea del Valle de Querétaro. Rev. Mex. Ciencias Geológicas 22, 1–18.

Carreón-Freyre, D., Cerca, M., Ochoa-González, G., Teatini, P., Zuñiga, F.R., 2016. Shearing along faults and stratigraphic joints controlled by land subsidence in the Valley of Queretaro. Hydrogeol. J. 24 (3), 657–674.

Carreon-Freyre, D.C., Cerca, M., 2006. Delineating the near-surface geometry of the fracture system affecting the Valley of Querétaro, Mexico: Correlation of GPR signatures and physical properties of sediments. Near Surf. Geophys. 4 (1), 49–55.

Carrera-Hernández, J.J., Carreón-Freyre, D., Cerca-Martínez, M., Levresse, G., 2016. Groundwater flow in a transboundary fault-dominated aquifer and the importance of regional modeling: the case of the city of Querétaro. Hydrogeol. J. 24 (2), 373–393. https://doi.org/10.1007/s10040-015-1363-x.

Castellazzi, P., Arroyo-Domínguez, N., Martel, R., Calderhead, A.I., Normand, J.C.L., Gárfias, J., Rivera, A., 2016. Land subsidence in major cities of Central Mexico: Interpreting InSAR-derived land subsidence mapping with hydrogeological data. Int. J. Appl. Earth Obs. Geoinf. 47, 102–111. https://doi.org/10.1016/j.jag.2015.12.002.

Castellazzi, P., Garfias, J., Martel, R., Brouard, C., Rivera, A., 2017. InSAR to support sustainable urbanization over compacting aquifers: The case of Toluca Valley, Mexico. Int. J. Appl. Earth Obs. Geoinf. 63, 33–44. https://doi.org/10.1016/j.jag.2017.06.011.

Castellazzi, P., Longuevergne, L., Martel, R., Rivera, A., Brouard, C., Chaussard, E., 2018. Quantitative mapping of groundwater depletion at the water management scale using a combined GRACE/InSAR approach. Remote Sens. Environ. 205. 10.1016/j.rse.2017.11.025.

CEA Querétaro, 2011. Estabilización y remediacíon del acuífero del Valle de Querétaro. Agua potable y Saneamiento, CEA, Gob. del Edo. de Qro., 24 p.

CEA Querétaro, 2016. Acueducto II. https://www.ceaqueretaro.gob.mx/cultura-del-agua/acueducto-ii/ (accessed 23 June 2021).

CEA Querétaro, 2017. Resumen comparativo de la puesta en marcha del sistema acueducto II. Agua potable y Saneamiento, CEA, Gob. del Edo. de Qro., 35 p.

Chaussard, E., Wdowinski, S., Cabral-Cano, E., Amelung, F., 2014. Land subsidence in central Mexico detected by ALOS InSAR time-series. Remote Sens. Environ. 140, 94–106. https://doi.org/10.1016/j.rse.2013.08.038.

Cigna, F., Osmanoğlu, B., Cabral-Cano, E., Dixon, T.H., Ávila-Olivera, J.A., Garduño-Monroy, V.H., DeMets, C., Wdowinski, S., 2012. Monitoring land subsidence and its induced geological hazard with Synthetic Aperture Radar Interferometry: A case study in Morelia, Mexico. Remote Sens. Environ. 117, 146–161. https://doi.org/10.1016/j.rse.2011.09.005.

Cigna, F., Tapete, D., 2021. Satellite InSAR survey of structurally-controlled land subsidence due to groundwater exploitation in the Aguascalientes Valley, Mexico. Remote Sens. Environ. 254, 112254. https://doi.org/10.1016/j.rse.2020.112254.

Crosetto, M., Monserrat, O., Cuevas-González, M., Devanthéry, N., Crippa, B., 2016. Persistent Scatterer Interferometry: A review. ISPRS J. Photogramm. Remote Sens. 115, 78–89. https://doi.org/10.1016/j.isprsjprs.2015.10.011.

Esteller, M.V., Diaz-delgado, CARLOS, 2002. Environmental effects of aquifer overexploitation: A case study in the highlands of Mexico. Environ. Manage. 29 (2), 266–278. https://doi.org/10.1007/s00267-001-0024-0.

Farina, P., Avila-Olivera, J.A., Garduño-Monroy, V.H., Catani, F., 2008. DInSAR analysis of differential ground subsidence affecting urban areas along the Mexican Volcanic Belt (MVB). Riv. Ital. di Telerilevamento (AIT), Telerilevamento a microonde. L'attività di Ric. e le Appl. 40, 103–113.

Ferretti, A., Prati, C., Rocca, F., 2001. Permanent scatterers in SAR interferometry. IEEE Trans. Geosci. Remote Sens. 39, 8–20. https://doi.org/10.1109/36.898661.

Galloway, D.L., Hoffmann, J., 2007. The application of satellite differential SAR interferometry-derived ground displacements in hydrogeology. Hydrogeol. J. 15 (1), 133–154.

Hancox, J., Gárfias, J., Aravena, R., Rudolph, D., 2010. Assessing the vulnerability of over-exploited volcanic aquifer systems using multi-parameter analysis, Toluca Basin, Mexico. Environ. Earth Sci. 59 (8), 1643–1660.

Hatch Kuri, G., 2017. Agua subterránea en México: retos y pendientes para la transformación de su gestión. In: Denzin, C., Taboada, F., Pacheco-Vega, R. (Eds.), El estado del agua en México. Actores, sectores y paradigmas para una transformación social-ecológica. Fundación Friedrich Ebert Stiftung-Proyecto Regional Transformación Social-Ecológica, Ciudad de México, pp. 149–170.

INEGI, 2011. Censo de Población y Vivienda 2010, INEGI, Mexico. https://sinegi.page.link/2sFa (accessed 23 June 2021).

Moreno, J., Marañón, B., Lopez, D., 2010. Los acuíferos sobreexplotados: origen, crisis y gestión social. In: Jiménez Cisneros, B., Torregrosa y Armentia, M.L., Aboites, L. (Editors): El agua en México, Cauces y Encauces (702 pp.). Mexico: Academia Mexicana de Ciencias, 1era edición, pp.79-115.

INEGI, 2021. Censo de Población y Vivienda 2020. INEGI, Mexico.

Ochoa-González, G.H., Carreón-Freyre, D., Cerca, M., López-Martínez, M., 2015. Assessment of groundwater flow in volcanic faulted areas. A study case in Queretaro, Mexico. Geofis. Int. 54 (3), 199–220. https://doi.org/10.1016/j.gi.2015.04.016.

Ochoa-González, G.H., Carreón-Freyre, D., Franceschini, A., Cerca, M., Teatini, P., 2018. Overexploitation of groundwater resources in the faulted basin of Querétaro, Mexico: A 3D deformation and stress analysis. Eng. Geol. 245, 192–206. https://doi.org/10.1016/j.enggeo.2018.08.014.

Ochoa-González, G.H., Carreón-Freyre, D., Teatini, P., Cerca, M., 2014. Urban structure damaged by differential land level lowering in the lacustrine plain of Queretaro City, Mexico. In: EGU General Assembly Conference Abstracts, p. 16632.

Osmanoğlu, B., Dixon, T.H., Wdowinski, S., Cabral-Cano, E., Jiang, Y., 2011. Mexico City subsidence observed with persistent scatterer InSAR. Int. J. Appl. Earth Obser. Geoinform. 13, 1–12. https://doi.org/10.1016/j.jag.2010.05.009.

Pacheco, J., Arzate, J., Rojas, E., Arroyo, M., Yutsis, V., Ochoa, G., 2006. Delimitation of ground failure zones due to land subsidence using gravity data and finite element modeling in the Querétaro valley, México. Eng. Geol. 84 (3-4), 143–160. https://doi.org/10.1016/j.enggeo.2005.12.003.

Pacheco-Martínez, J., Cabral-Cano, E., Wdowinski, S., Hernández-Marín, M., Ortiz-Lozano, J.Á., Zermeño-de-León, M.E., 2015a. Application of InSAR and Gravimetry for Land Subsidence Hazard Zoning in Aguascalientes, Mexico. Remote Sens. 10.3390/rs71215868.

Pacheco-Martínez, J., Wdowinski, S., Cabral-Cano, E., Hernández-Marín, M., Ortiz-Lozano, J.A., Oliver-Cabrera, T., Solano-Rojas, D., Havazli, E., 2015. Application of InSAR and gravimetric surveys for developing construction codes in zones of land subsidence induced by groundwater extraction: case study of Aguascalientes, Mexico. Proc. Int. Assoc. Hydrol. Sci. 372, 121–127.

Rudolph, D.L., Sultan, R., Garfias, J., McLaren, R.G., 2006. Significance of enhanced infiltration due to groundwater extraction on the disappearance of a headwater lagoon system: Toluca Basin, Mexico. Hydrogeol. J. 14 (1-2), 115–130. https://doi.org/10.1007/s10040-005-0463-4.

Solano-Rojas, D., Cabral-Cano, E., Hernández-Espriú, A., Wdowinski, S., DeMets, C., Salazar-Tlaczani, L., Falorni, G., Bohane, A., 2015. La relación de subsidencia del terreno InSAR-GPS y el abatimiento del nivel estático en pozos de la zona Metropolitana de la Ciudad de México. Boletín la Soc. Geológica Mex.

Sowter, A., Bin Che Amat, M., Cigna, F., Marsh, S., Athab, A., Alshammari, L., 2016. Mexico City land subsidence in 2014–2015 with Sentinel-1 IW TOPS: Results using the Intermittent SBAS (ISBAS) technique. Int. J. Appl. Earth Obs. Geoinf. 52, 230–242. https://doi.org/10.1016/j.jag.2016.06.015.

Suárez, G., Jaramillo, S.H., López-Quiroz, P., Sánchez-Zamora, O., 2018. Estimation of ground subsidence in the city of Morelia, Mexico using Satellite Interferometry (INSAR) s. Geofísica Int. 57, 39–58.

Takaku, J., Tadono, T., Tsutsui, K., 2014. Generation of high-resolution global DSM from ALOS PRISM ISPRS Ann. Photogramm. Remote Sens. Spat. Inf. Sci. 2.

Terzaghi, K., 1925. Principles of soil mechanics, IV - Settlement and consolidation of clay. Eng. News-Record 95, 874–878.

Villa Alvarado, C.J., Delgadillo-Ruiz, E., Mastachi-Loza, C.A., González-Sosa, E., Norma Maricela, R.S., 2014. A Physically Based Runoff Model Analysis of the Querétaro River Basin. J. Appl. Math. 2014, 1–12.